# Transceivers and Spectrum Usage Minimization in Few-Mode Optical Networks

Cristina Emma Margherita Rottondi D, Paolo Martelli D, Pierpaolo Boffi D, and Massimo Tornatore D

Abstract—Metro-area networks are likely to create the right conditions for the deployment of few-mode transmission (FMT) due to limited metro distances and rapidly increasing metro traffic. To address the new network design problems arising with the adoption of FMT, integer linear programming (ILP) formulations have already been developed to optimally assign modulation formats, baud rates, and transmission modes to lightpaths, but these formulations lack scalability, especially when they incorporate accurate constraints to capture inter-modal coupling. In this paper, we propose a heuristic approach for the routing, modulation format, baud rate and spectrum allocation in FMT networks with arbitrary topology, accounting for inter-modal coupling and for distanceadaptive reaches of few-mode (specifically, up to five modes) signals generated by either full multi-in multi-out (MIMO) or lowcomplexity MIMO transceivers and for two different switching scenarios (i.e., spatial full-joint and fractional-joint switching). In our illustrative numerical analysis, we first confirm the quasioptimality of our heuristic by comparing it to the optimal ILP solutions, and then we use our heuristic to identify which switching scenario and FMT transceiver technology minimize spectrum occupation and transceiver costs, depending on the relative costs of transceiver equipment and dark fiber leasing.

Index Terms—Few-mode optical fibers, inter-modal crosstalk, mode and spectrum assignment.

# I. INTRODUCTION

EW-Mode Transmission (FMT) is a promising Space Division Multiplexing (SDM) solution [1] that, in principle, can scale the capacity of an optical fiber by a factor equal to the number of co-propagating modes. FMT is expected to find an initial application especially in metro areas, as it promises to provide a boost to fiber capacities over relatively-short metro distances while maintaining low fiber-manufacturing cost. However, in practical settings, such capacity boost is

Manuscript received December 13, 2018; revised February 7, 2019; accepted February 18, 2019. Date of publication February 25, 2019; date of current version July 31, 2019. The work of M. Tornatore was supported by the National Science Foundation under Grant 1716945. (Corresponding author: Cristina Emma Margherita Rottondi.)

- C. E. M. Rottondi is with the Dipartimento di Elettronica e Telecomunicazioni, Politecnico di Torino, Turin 10129, Italy (e-mail: cristina.rottondi @polito.it).
- P. Martelli and P. Boffi are with the Dipartimento di Elettronica, Informazione e Bioingegneria, Politecnico di Milano, Milan 20133, Italy (e-mail: paolo.martelli@polimi.it; pierpaolo.boffi@polimi.it).
- M. Tornatore is with the Dipartimento di Elettronica, Informazione e Bioingegneria, Politecnico di Milano, Milan 20133, Italy, and also with the University of California, Davis, CA 95616 USA (e-mail: massimo.tornatore@polimi.it).

Color versions of one or more of the figures in this paper are available online at http://ieeexplore.ieee.org.

Digital Object Identifier 10.1109/JLT.2019.2900852

limited by mode coupling that, due to the differential mode group delay (DMGD) [2], can dramatically reduce the reach in FMT, to the point that it might decrease or even neutralize the capacity gains introduced by parallel mode transmissions over a single channel. In this study, we observe how the trade-off between capacity and reach varies significantly depending on whether: i) the signal is optically switched using either full-joint or fractional-joint switching of the spatial mode dimension; ii) FMT is implemented through low-complexity or high-complexity MIMO. Identifying which combinations of the above-mentioned switching and MIMO options leads to the minimum-cost solution is not a trivial task and requires to solve a Routing and Spectrum Assignment (RSA) problem. In particular, if the fiber spectrum is assumed to be managed through a flexi-grid, solving the RSA problem with FMT requires the joint optimization of several transmission/networking parameters, namely we must assign to each lightpath one or multiple groups of modes, the right number of adjacent spectrum slots, the right transceiver baud rate and modulation format.

In our previous study [2], we addressed the problem of Routing, Modulation format, Baud rate and Spectrum Allocation (RMBSA) in flexi-grid metro rings using Integer Linear Programming (ILP). However, ILP lacks scalability in case of larger and more practical topologies. In this paper we propose a scalable heuristic algorithm to solve the RMBSA problem. Though several studies on resource allocation in SDM flexigrid networks have recently appeared [3], to the best of our knowledge, this is the first attempt to i) account for reach impairments due to inter-modal coupling and ii) consider multiple baud rates and modulation formats in the design of a heuristic approach for RMBSA with FMT. Using our proposed heuristic, in this paper we assess FMT benefits in terms of spectrum and transceiver costs, comparing two transceiver architectures (adopting either full MIMO or low-complexity MIMO technology) and two switching paradigms (i.e., spatial full-joint and fractional-joint switching) on practical-scale networks and we evaluate the switching and transmission options leading to the lowest overall expenditures, under different assumptions on dark fiber leasing and transceiver equipment costs.

The remainder of this paper is organized as follows. Section II briefly overviews the related literature. In Section III we describe our assumptions on the network and transceiver models. The

<sup>1</sup>A preliminary version of this paper appears in [4]. With respect to [4], this paper considers multiple transmission technologies and switching scenarios. Moreover, we provide a detailed description of our heuristic approach, an extensive performance assessment and a cost evaluation depending on transceiver equipment and dark fiber leasing costs.

heuristic approach used to solve the RMBSA problem with FMT is presented in Section IV and numerically assessed in Section V. Conclusions are drawn in Section VI.

#### II. RELATED WORK

The RSA problem has been recently investigated for different SDM technologies, mainly for multi-core transmission (MCT), FMT and for the case of bundles of fibers. The reader is referred to [3] for a survey on resource allocation schemes and algorithms for SDM networking. Solutions for resource optimization, control and planning have appeared in [5]-[10], where three different switching approaches for SDM networks are proposed: i) in independent spatial/spectral switching, demands can be freely switched in both space and spectrum domains without constraints; ii) in spatial full-joint switching only spectral flexibility is allowed, whereas the spatial dimension must be switched as a whole; iii) in spatial fractional-joint switching sub-groups of spatial resources are switched together as independent units. These three approaches are compared in [10]–[12] for SDM with fiber bundles. Our proposed heuristic approach is designed for spatial fractional-joint and full-joint switching in FMT, but it can be easily adapted to the case of *independent switching*.

A few existing studies have proposed ILPs and heuristics for the RSA problem with MCT/FMT. Refs. [13]-[16] solve the Routing, Wavelength and Core Assignment problem in MCT using ILP, based on simplifying worst-case approximations on the impact of crosstalk. In [17], inter-core crosstalk is explicitly modeled to evaluate the impact of MIMO-based crosstalk suppression. Several optimization objectives are possible as, e.g., minimizing the maximum allocated slice number over the whole network [15] or minimizing the overall network cost due to switching modules required for different cores at the input/output links of optical crossconnects [16]. Our proposed heuristic minimizes either the overall spectrum occupation or the cost of the installed transceivers. An ILP for CapEx minimization in a flexi-grid FMT network is proposed also in [18], under the assumption of spatial full-joint switching. In our previous work [2], we developed an ILP for the RMBSA problem and we provided as an input to this problem the transmission reach values associated to different modulation formats, baud rates, and number of modes considering a 5-mode fiber with spatial full-joint switching and spatial fractional-joint switching. In this paper, we will consider both switching approaches, but our transmission model will be extended to consider also the case of full MIMO transceivers.

Heuristic algorithms for SDM networks have been proposed in [19]–[22] for spectrum and core allocation with dynamic traffic. The proposed methods are based on core/spectrum prioritization criteria, that privilege the assignment of traffic requests to non-adjacent cores or to non-overlapping spectrum portions in adjacent cores. Refs. [23], [24] apply dynamic routing, spectrum, spatial mode and modulation format assignment algorithms to evaluate the blocking probability in a FMT network using orbital angular momentum states with either *full-joint* and *fractional-joint* switching approaches. However, the heuristic algorithms in [23], [24] do not consider the additional filtering penalties introduced by FMT transmission in case of *fractional-joint* switching, whereas our transmission model and

node architecture account for the presence of an optical demultiplexer and multiplexer to separate and recombine the mode groups at every intermediate node traversed by the lightpath. Moreover, inter-modal crosstalk among mode groups is also taken into account by our model when lightpaths transmitting over separate mode groups share the same spectrum channel. Such assumptions have a remarkable impact on the complexity of the routing and spectrum assignment criteria. Consider the case of two lightpaths with some common links, transmitting over different mode groups along the same optical channel. Consider then the same two lightpaths, allocated over two separate channels. Under our assumptions, in the first scenario transmission impairments are higher than in the second due to crosstalk among mode groups, which cause a decrease of transmission reaches. Conversely, in [23], [24] the two scenarios are equivalent in terms of crosstalk impairments. It follows that, under the assumptions of [23], [24], the mode and spectrum allocation problem can be treated as a 2D strip packing problem [25] (i.e., the problem of allocating rectangles of different sizes inside a given area), whereas under our assumptions such approach is not viable, as packing two rectangles (i.e., lightpaths) along the spatial dimension may lead to higher bandwidth requirements to accommodate additional transceivers to satisfy the traffic demand (which would increase the rectangle size).

#### III. TRANSMISSION AND NETWORK MODEL

# A. Transceiver Model

As crosstalk among modes can be cancelled by means of MIMO processing [26], in this paper we adopt a full-MIMO transceiver scheme as shown in Fig. 1, where FMT-SDM with a number M of spatial modes equal to 5 is considered, combined to Polarization Division Multiplexing (PDM), i.e, transmission of two polarization modes for each spatial mode. Such a full-MIMO transceiver requires a  $2M \times 2M$ Digital-Signal-Processing (DSP), hence composed by  $4M^2$  basic equalizers [26] and we consider this number of equalizers as a complexity (and, hence, cost) factor. So the complexity factor of the full-MIMO transceiver scales according to a square law with M, hence in our case it is 25 times the complexity of the Single Mode Transmission (SMT) transceiver. We assume that crosstalk cancellation by full-MIMO DSP at the receiver enables the same reach for FMT and SMT. Note that, since full-MIMO DSP requires that all the spatial modes of the same wavelength follow the same path between transmitter and receiver [27], the only possible switching approach for full-MIMO transceiver scheme is the spatial full-joint switching. We also consider a few-mode transceiver with reduced complexity, as described in [2] (see Fig. 2), based on the hybrid optical/digital mode separation proposed in [28], [29]: using an optical demultiplexer to separate mode groups, at maximum 4 × 4 MIMO is employed per mode group to discriminate the strongly-coupled nearly-degenerate modes of the same group. Therefore, coupling among mode groups induced by the propagation sets the most significant limitation to the transmission reach achievable for a given optical signal-to-noise ratio (OSNR) budget, as evidenced by the reach calculations reported in [2]. In the few-mode transceiver, an optical de/multiplexer is

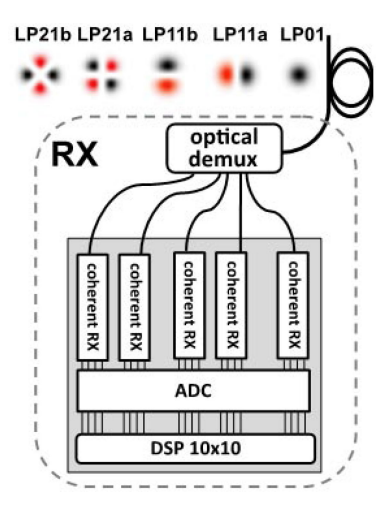


Fig. 1. The full-MIMO few-mode transceiver architecture.

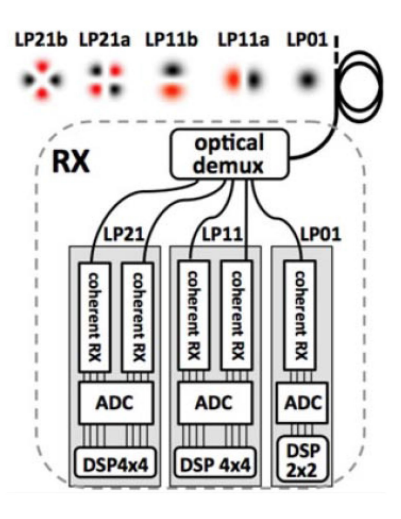


Fig. 2. The low-complexity MIMO few-mode transceiver architecture described in [2].

employed to separate/combine the mode groups at the two end nodes of the lightpath, then the degenerate modes inside each group and their polarizations are digitally demultiplexed after coherent detection. In case of 5 spatial modes grouped in three different groups, as shown in Fig. 2, the number of basic equalizers of the low-complexity MIMO transceiver is 36, giving a complexity factor 9 times the SMT transceiver complexity, which is only 9/25 times the full-MIMO transceiver complexity. Note that the low-complexity MIMO transceiver enables the adoption of fractional-joint switching, as an alternative to the full-joint switching. In case of fractional-joint switching, an optical demultiplexer and an optical multiplexer are also required to separate and recombine the mode groups at every intermediate node. Therefore, an EDFA has to be introduced after the node to compensate losses. In addition, according to the reach calculations reported in [2], mode separation and recombination introduce a reach penalty of 100 km for each intermediate node traversed by lightpath. In our illustrative numerical analysis, we will also consider a fractional-joint switching scenario in which node traversal penalties are disregarded, envisioning future advancements in the mode switching technologies.

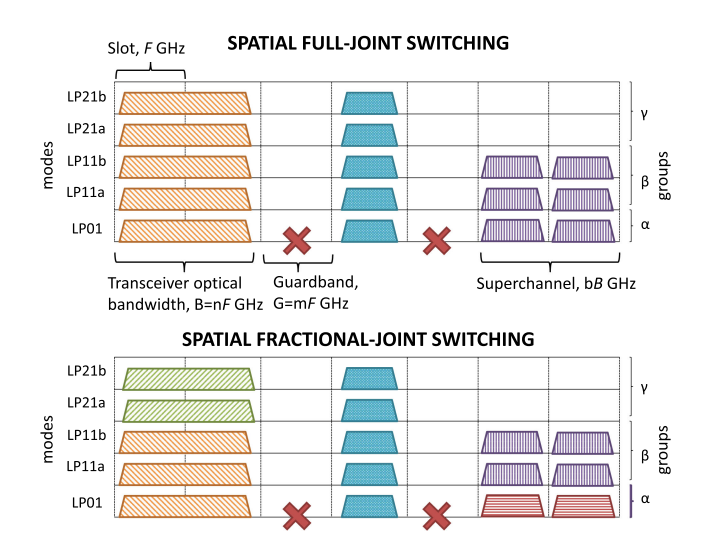


Fig. 3. Spatial full-joint vs. fractional-joint switching scenarios.

TABLE I
LIST OF ALLOWED MODE GROUP COMBINATIONS

| Switching   | Allowed group  | Allowed channel sharing options   |
|-------------|--|---|
| scenario    | combinations   |   |
| Full-joint  | $\alpha; \alpha \cup \beta; \alpha \cup \beta \cup \gamma$ | -   |
| Fractional- | $\alpha; \beta; \gamma; \alpha \cup \beta;$                | $\alpha$ and $\beta$ ; $\alpha$ and $\gamma$ ; $\beta$ and $\gamma$ ; $\alpha$ and $\beta$ and                    |
| joint       | $\beta \cup \gamma; \alpha \cup \gamma; \alpha \cup \beta$ | $\gamma$ ; $\alpha \cup \beta$ and $\gamma$ ; $\alpha \cup \gamma$ and $\beta$ ; $\alpha$ and $\beta \cup \gamma$ |
|             | $\beta \cup \gamma$  |   |

#### B. Network Model

The network physical topology under consideration is represented as a graph  $\mathcal{G}=(\mathcal{N},\mathcal{E})$ , where  $\mathcal{N}$  is the node set and  $\mathcal{E}=(i,j)\in\mathcal{N}\times\mathcal{N}$  is the set of links connecting nodes i and j. Links are assumed to be bidirectional (i.e.  $(i,j)\in\mathcal{E}\Rightarrow(j,i)\in\mathcal{E}$ ) and support 5-mode-transmission [29] (namely the fundamental LP01 and two pairs of spatially degenerate modes LP11a/LP11b and LP21a/LP21b, where each mode supports polarization multiplexing). Modes are assembled into three groups: group  $\alpha$  comprises the LP01 mode, group  $\beta$  the LP11a and LP11b modes, group  $\gamma$  the LP21a and LP21b modes.

As depicted in Fig. 3, we assume that the optical spectrum is divided in a grid of frequency slots of granularity  $F=12.5\,\mathrm{GHz}$ . As defined in the ITU-T standard [30], the nominal central frequency is placed in the middle of the slot, so that optical carriers can be located along a predefined grid with  $F/2\,\mathrm{GHz}$  spacing. The total spectrum per link is  $S=kF\,\mathrm{GHz}$  (with k integer).

If a traffic request exceeds the capacity of a single transceiver, it can be served by a number b of adjacent transceivers forming a superchannel, which is handled and switched as a single entity [31], given that it is separated from the adjacent (super)channels by a guardband of G=mF GHz (with m integer) to avoid overlap and crosstalk among neighbor signals (in Fig. 3, a 1 slot guardband is assumed). The superchannel bandwidth can be computed as bB, where B=nF is the transceiver optical bandwidth, expressed as integer multiple of the slot width. Such bandwidth depends on the transceiver baud rate. Transceivers can work at two baud rates (B=14 or B=28 GBd, thus occupying transceiver slots of 2F=25 GHz or 3F=37.5 GHz, respectively) and support different modulation formats (i.e. DP-

| Symbol                                     | Description   | Symbol  | Description  |
|--|---|---|--|
| $\mathcal{G} = (\mathcal{N}, \mathcal{E})$ | network graph, with ${\cal N}$ being the set of nodes and       | $\mathcal{O} = \{\alpha, \beta, \gamma\}$             | set of mode groups   |
|  | $\mathcal E$ being the set of links                             |   |  |
| $\mathcal{H}$                              | set of transceiver baud rates                                   | M   | set of possible modulation formats   |
| S  | set of spectrum slots of each link                              | $\mathcal{T}$   | set of source-destination node pairs $(s, d)$ : $t_{sd} > 0$                   |
| $\mathcal{J} = \{0, 1, 2, \dots\}$         | set of possible number of intermediate nodes tra-               | $C = \{\alpha, \beta, \alpha \cup \}$                 | set of mode group combinations   |
|  | versed by a lightpath (the highest integer value                | $\beta, \gamma, \beta \cup \gamma, \alpha \cup \beta$ |  |
|  | depends on the network topology)                                | $\gamma, \alpha \cup \beta \cup \gamma$               |  |
| $C_{occ}$                                  | set of mode groups occupied over lighpath $k$ (either           | $\mathcal{K}_{sd}$                                    | set of candidate lightpaths between source node $s$ and                        |
|  | for transmission over $k$ itself or over other light-           |   | destination node $d$ such that $(s,d) \in \mathcal{N} \times \mathcal{N}$      |
|  | paths sharing the same channel of $k$ on at least one           |   |  |
|  | of its links)   |   |  |
| $A^{sd} = [a_{nn'k}]$                      | boolean parameters set to 1 if link $(n, n')$ belongs           | $R = r_{mh}$  | capacity of one transceiver operating at baud rate h                           |
|  | to lightpath $k \in \mathcal{K}_{sd}$                           |   | with modulation format m   |
| $l_k$                                      | physical length of lightpath $k$ (km)                           | $T = [t_{sd}]$  | traffic matrix between source-destination node pairs                           |
|  |   |   | (Gb/s)   |
| G  | guardband width (GHz), expressed as a multiple of               | $\mathcal{F} = [F_h]$                                 | optical bandwidth of transceiver with band rate $h$ ,                          |
|  | F   |   | expressed as a multiple of $F$   |
| $L^x = [l^x_{mhCj}]$                       | maximum reach of modulation format $m$ using                    | $\Psi = [\psi_{mch}]$                                 | cost of one transceiver operating at baud rate $h$ , mod-                      |
|  | baud rate $h$ transmitting over mode group(s) in                |   | ulation format $m$ and transmitting over mode group(s)                         |
|  | combination $C \in \mathcal{C}$ and traversing $j$ intermediate |   | in combination $C \in \mathcal{C}$ . For low-complexity MIMO                   |
|  | nodes (km)  |   | transceivers it is computed as $\Delta( C  + \sum_{o \in C} (\rho_o^2 - 1)^2)$ |
|  |   |   | $1)\delta$ ), where $\Delta$ is the cost of a single-mode transceiver          |
|  |   |   | and $\delta \leq 1$ is a non-negative tunable multiplicative                   |
|  |   |   | factor, whereas for 5-modes full-MIMO transceivers it                          |
|  |   |   | is computed as $\Delta(1+24\delta)$  |
| $\rho_o$                                   | number of modes in group $o \in \mathcal{O}$                    | $p_x$   | maximum cardinality of sets $\mathcal{K}_{sd}$                                 |
| $\Phi = [\phi_{nn'o}]$                     | boolean parameters set to 1 if mode group $o \in \mathcal{O}$   |   |  |
|  | is occupied over link $(n, n')$                                 |   |  |

TABLE II LIST OF SETS AND PARAMETERS

QPSK and DP-n-QAM, with n=8,16,32,64). Depending on the switching scenario, transceivers may transmit over different combinations of mode groups (Table I reports the allowed combinations). In the remainder of this paper, for low-complexity MIMO transceivers we will adopt the transmission reaches reported in [2, Table II] for each feasible choice of mode group(s), baud rate, modulation format and number of intermediate nodes traversed by the lightpath. For full-MIMO transceivers operating over groups  $\alpha \cup \beta \cup \gamma$ , the reaches of low-complexity MIMO transceivers operating over group  $\alpha$  reported in [2, Table II] will be adopted, disregarding node traversal penalties.

Moreover, in the fractional-joint switching scenario, spectrum (super)channels may be shared by multiple lightpaths, given that each of them occupy different mode group(s) and that the total spectral width of their occupied transceiver slots does not exceed the (super)channel width (see Fig. 3, bottom). Table I also reports how the mode groups can be attributed to lightpaths sharing the same (super)channel. Note that coexistence of two or three lightpaths is allowed: in the former case, each lightpath may occupy one mode group, or one of the two lightpaths may occupy two mode groups (e.g.,  $\alpha \cup \beta$ ,  $\alpha \cup \gamma$  or  $\beta \cup \gamma$ ). In the latter case, each of the three lightpaths occupies a single mode group.

Note that, in our heuristic algorithm, the computation of transmission impairments due to channel sharing in the fractional-joint switching scenario follows a conservative approach: if two (or more) lightpaths share a channel on at least one link, the reaches of their modulation formats are computed assuming that transmission occurs over the whole set of occupied groups (e.g., if lightpath 1 transmits over group  $\alpha$  and lightpath 2 transmits over group  $\beta$ , we compute the reaches of their respective baud rates and modulation formats assuming that they both transmit over groups  $\alpha \cup \beta$ ).

# IV. A HEURISTIC ALGORITHM FOR THE RMBSA PROBLEM WITH FMT

# A. Problem Definition

Given an arbitrary network topology and a traffic matrix defining the amount of traffic to be transmitted between every node pair of the network, the RMBSA problem consists in:

- assigning to every traffic flow a lightpath connecting its source and destination nodes;
- allocating a channel for each lightpath, ensuring spectral continuity along the traversed links, as well as spectral contiguity between spectrum slots associated to the same lightpath and separation of spectrally adjacent channels by means of guardbands;
- attributing mode groups used for transmission to every lightpath;
- choosing a combination of baud rate and modulation format for the transceivers serving each lightpath.

We consider two different objectives, i.e., the minimization of the cost of the transceivers to be installed or of the overall spectrum occupation (i.e. the total amount of occupied spectrum slots over all the network links).

# B. Algorithm Description

We now describe our proposed heuristic algorithm to solve the RMBSA problem (see Alg. 1). The logical flow of the procedures implemented by the algorithm is reported in Fig. 4. The algorithm uses lists to store in each entry one candidate assignment of lightpath, baud rate, modulation format and mode group(s) for a given set of source-destination node pairs (s,d). In order to store such information, an entry includes several fields, each containing one specific attribute. Attributes can be

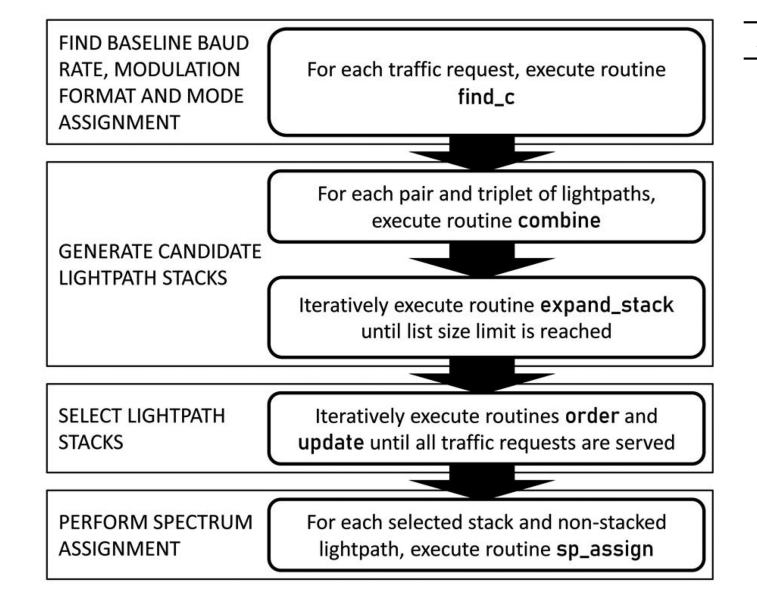


Fig. 4. Logical flow of the procedures implemented by the heuristic algorithm for PMBS A

numbers (e.g., the transceiver baud rate), strings of characters (e.g., the adopted modulation format), sets (e.g., the set of mode group(s) used for transmission), or more complex structures (e.g., sequences of links and nodes that identify a lightpath). In the remainder of the Section, we will indicate the field  $\mathtt f$  of list  $\mathtt L$  as  $\mathtt L$ .  $\mathtt f$  and the  $\mathtt i$ -th entry of list  $\mathtt L$  as  $\mathtt L$  ( $\mathtt i$ ). Moreover, we indicate the length of list  $\mathtt L$  as  $len(\mathtt L)$ . Table II lists the symbols used in this section.

For each traffic request  $t_{sd}$ , using the routine find\_c, the algorithm first identifies a set of at most  $p_x$  shortest paths<sup>2</sup> connecting the source node s to the destination node d (Alg. 1, lines 2–4). Then, for each path, the find c routine considers every combination of modulation format  $m \in \mathcal{M}$ , band rate  $h \in \mathcal{H}$ , set of mode group(s)  $C \in \mathcal{C}$  and set of overall occupied mode groups  $C_{occ} \in \mathcal{C}$  (Alg. 2, line 4–7). Using two separate parameters C and  $C_{occ}$  captures scenarios where multiple lightpaths share the same spectrum channel: for example, we may consider a lightpath transmitting over group  $\alpha$  and sharing its channel (on at least one of its links) with another lightpath transmitting over group  $\beta$ , thus having  $C = \{\alpha\}$  and  $C_{occ} = \{\alpha \cup \beta\}$ . Note that only combinations such that  $C \subseteq C_{occ}$  are feasible and that the knowledge of  $C_{occ}$  is necessary for the reach computations. For each combination, the number of intermediate nodes jtraversed by lightpath k is computed (Alg. 2, line 5). If the length of lightpath k does not exceed the maximum reach  $l^x_{mhC_{acc}j}$  of a transceiver operating at baud rate h and modulation format m over mode group(s)  $C_{occ}$  (not C!) and traversing j intermediate nodes, then the number Tx of transceivers necessary to serve the traffic demand  $t_{sd}$ , their total cost CT and the corresponding total spectrum occupation SP are calculated (Alg. 2, lines 6-8). Moreover, mode occupation over each link of the network is tracked by setting the boolean indicator  $\phi_{nn'o}$ to 1 if mode group  $o \in \mathcal{O}$  is used for transmission over link (n, n') belonging to lightpath  $k \in \mathcal{K}_{sd}$ , thus filling the matrix

```
Algorithm 1: Solve RMBSA.
       1: On input of
                       \mathcal{G}=(\mathcal{V},\mathcal{E}),\mathcal{O},\mathcal{C},\mathcal{H},\mathcal{M},\mathcal{F},\Psi,\mathcal{S},\mathcal{T},G,T,R,L^x
       2: for all (s,d) \in \mathcal{T} do
                              [\Gamma_{sd}, B_{sd}] \leftarrow
                    \texttt{find\_c}(\mathcal{G}, \mathcal{O}, \mathcal{C}, \mathcal{H}, \mathcal{M}, \mathcal{F}, \Psi, G, R, L^x, (s, d), t_{sd})
       4: end for
       5: Initialize empty list \Gamma
       6: for all (s_1, d_1), (s_2, d_2) \in \mathcal{T} \times \mathcal{T} do
                          St_2 \leftarrow \mathtt{combine}(\mathcal{G}, \mathcal{O}, \mathcal{F}, G, \mathcal{I} = \{1, 2\},
                              \Gamma_{s_1d_1},\Gamma_{s_2d_2}
                            Append list St_2 to list \Gamma
      9: end for
       10: for all (s_1, d_1), (s_2, d_2), (s_3, d_3) \in \mathcal{T} \times \mathcal{T} \times \mathcal{T} do
                                   St_3 \leftarrow \mathtt{combine}(\mathcal{G}, \mathcal{O}, \mathcal{F}, G, \mathcal{I} = \{1, 2, 3\}, \Gamma_{s_1 d_1}, \mathcal{O}, \mathcal{O}, \mathcal{F}, \mathcal{O}, 
                                   \Gamma_{s_2d_2},\Gamma_{s_3d_3}
       12:
                                   Append list St_3 to list \Gamma
       13: end for
       14: initialize empty list \Gamma_{fin} and list \Gamma_{curr} \leftarrow \Gamma
       15: while len(\Gamma_{curr}) > 0 and len(\Gamma_{curr}) < Th do
                                   initialize empty list \Gamma_{next}
       17:
                                   for all entries \Gamma_{curr}(w): 1 \leq w \leq len(\Gamma_{curr}),
                                   (s,d) \in \mathcal{T} s.t. (s,d) is not already included
                                  in entry \Gamma_{curr}(w) do
       18:
                                       \Gamma_{new} \leftarrow
                                      expand_stack(\mathcal{G}, \mathcal{O}, \mathcal{C}, \mathcal{M}, R, G, \Gamma_{curr}(w), \Gamma_{sd})
       19:
                                        Append list \Gamma_{new} to list \Gamma_{next}
       20:
                                   end for
       21:
                                    Append list \Gamma_{curr} to list \Gamma_{fin}, \Gamma_{curr} \leftarrow \Gamma_{next}
       22: end while
       23: \Gamma_{fin} \leftarrow \operatorname{order}(\Gamma_{fin}, \Gamma_{sd} : (s, d) \in \mathcal{T})
       24: Initialize empty list Ch and set \mathcal{Z} \leftarrow \emptyset
       25: while \Gamma_{fin} \neq \emptyset and T \setminus \mathcal{Z} \neq \emptyset do
                                   Append entry \Gamma_{fin}(1) to list Ch
       26:
                                   for all lightpaths i in stack stored in entry \Gamma_{fin}(1) do
       27:
       28:
                                        \mathcal{Z} \leftarrow \mathcal{Z} \cup \Gamma_{fin}.(s_i, d_i)(1)
       29:
                                   end for
                                   \Gamma_{fin} \leftarrow \mathtt{update}(\Gamma_{fin}, \Gamma_{fin}(1))
       30:
       31: end while
       32: for all entries Ch(w): 1 \leq w \leq len(Ch) do
       33:
                                    sp_assign(Ch(w), S)
       34: end for
```

 $\Phi = [\phi_{nn'o}]$  (lines 9-11). Note that the most spectrally efficient combination of baud rate, modulation format and mode group is stored in  $B_{sd}$  as baseline assignment (lines 12-14). Finally, the entry  $[k, CT, SP, m, h, Tx, C, C_{occ}, \Phi]$  is appended to the list  $\Gamma_{sd}$  of feasible assignments for request  $t_{sd}$  (line 15). At the end, the routine find\_c returns the list  $\Gamma_{sd}$  and the baseline assignment  $B_{sd}$  (Alg. 2, line 18).

35: for all  $(s,d) \in \mathcal{T} \setminus \mathcal{Z}$  do

 $sp_assign(B_{sd}, S)$ 

36:

**37: end for** 

Then, the algorithm considers the entries of the lists  $\Gamma_{sd}$  for every pair  $(s_1, d_1), (s_2, d_2)$  (resp. triplet  $(s_1, d_1), (s_2, d_2), (s_3, d_3)$ ) of traffic requests and checks whether they could share the same channel (Alg. 1, line 5-13). This is done

 $<sup>^2{\</sup>rm If}$  the network topology does not allow for  $p_x$  distinct lightpaths between (s,d), all the available lightpaths are returned.

## Algorithm 2: Find\_c.

```
1: On input of \mathcal{G}, \mathcal{O}, \mathcal{C}, \mathcal{H}, \mathcal{F}, \mathcal{M}, \Psi, R, L^x, G, (s, d), t_{sd}
2: Initialize empty list \Gamma_{sd} and Bm \leftarrow \infty
3: Find a set \mathcal{K}_{sd} of at most p_x shortest lightpaths from s
4: for all
k \in \mathcal{K}_{sd}, m \in \mathcal{M}, h \in \mathcal{H}, C \in \mathcal{C}, C_{occ} \in \mathcal{C} : C \subseteq C_{occ} do 5: j \leftarrow \left(\sum_{n,n'} A^{sd}_{nn'k}\right) - 1
6:
           Find minimum integer Tx: r_{mh}Tx \sum_{o \in C} \rho_o \geq t_{sd}
7:
           CT \leftarrow 2\psi_{mch}Tx, SP \leftarrow \sum_{(n,n') \in \mathcal{E}} a_{nn'k}(F_hTx + G)
8:
           for all (n, n') \in \mathcal{E}: A^{sd}_{nn'k} = 1, d \in \mathcal{D}: d \in C do
9:
                 \phi_{nn'o} \leftarrow 1
10:
              end for
11:
12:
              if SP < Bm then
               Bm \leftarrow SP, B_{sd} \leftarrow [k, CT, SP, m, h, Tx, C, C_{occ}, \Phi]
13:
14:
15:
             Append entry [k, CT, SP, m, h, Tx, C, C_{occ}, \Phi] to
            list \Gamma_{sd}
16: end if
17: end for
18: return \Gamma_{sd}, B_{sd}
```

# Algorithm 3: Combine.

```
1: On input of \mathcal{G}, \mathcal{O}, G, \mathcal{I}, \Gamma_{s_i d_i} : i \in \mathcal{I}
2: Initialize empty list St
3: for all combinations of entry indexes W = \{w_i\} : i \in \mathcal{I},
      1 \leq w^i \leq len(\Gamma_{s_i d_i}) identifying entries \Gamma_{s_i d_i}(w^i)
      such that \sum_{(n,n'\in\mathcal{E})} \prod_{i\in\mathcal{I}} A_{nn'\Gamma_{s_id_i}\cdot k(w^i)} \geq 0 and
      \sum_{i} \Gamma_{s_i d_i} . \phi_{nn'o}(w^i) \leq 1 \ \forall \ (n, n') \in \mathcal{E}, o \in \mathcal{O} \ \mathbf{do}
           compute SP_{tot} = \sum_{(n,n') \in \mathcal{E}} \max_i A_{nn'\Gamma_{s;d_i}.k(w^i)}.
          (\Gamma_{s_i d_i} . Tx(w^i) \cdot F_{\Gamma_{s_i d_i} . h(w^i)} + G)
           \begin{array}{l} \textbf{if } SP_{tot} < \sum_{i} \Gamma_{s_i d_i}.SP(w^i) \textbf{ then} \\ RSP \leftarrow \frac{\sum_{i} \Gamma_{s_i d_i}.SP(w^i) - SP_{tot}}{\sum_{i} \Gamma_{s_i d_i}.SP(w^i)} \end{array}
5:
6:
               \Phi_{tot} \leftarrow \sum_{i} \Gamma_{s_i d_i} . \Phi(w^i)
CT_{tot} \leftarrow \sum_{i} \Gamma_{s_i d_i} . CT(w^i)
7:
8:
               Append to list St entry
9:
               [[(s_i, d_i), \Gamma_{s_i d_i}.k(w^i), \Gamma_{s_i d_i}.m(w^i), \Gamma_{s_i d_i}.h(w^i),
              \Gamma_{s_i d_i} . c(w^i), \Gamma_{s_i d_i} . SP(w^i) : i \in \mathcal{I}, c_{occ}, SP_{tot},
               CT_{tot}, RSP, \Phi_{tot}
10:
               end if
11: end for
12: return St
```

by means of the routine combine, which takes as input the list  $\Gamma_{s_id_i}$  of feasible assignments for each of the two (resp. three) traffic requests  $(s_i,d_i):i\in\mathcal{I}$  (Note that  $\mathcal{I}$  defines a set of indexes for either pairs or triplets, i.e.,  $\mathcal{I}=\{1,2\}$  in the case of pairs and  $\mathcal{I}=\{1,2,3\}$  in the case of triplets). The routine explores every combination of pairs (resp. triplets) of list entries (one for each of the considered  $(s_i,d_i)$ ) having the same value of  $C_{occ}$ : if the two (resp. three) lightpaths stored in such entries share at least one link (i.e.,  $\sum_{(n,n')\in\mathcal{E}}\prod_{i\in\mathcal{I}}A_{nn'\Gamma_{s_id_i}.k(w^i)}\geq 0$ , where  $w^i$  is the index of the w-th entry of list  $\Gamma_{s_id_i}$ ) and each

# Algorithm 4: Expand\_Stack.

```
1: On input of \mathcal{G}, \mathcal{O}, G, \Gamma_{curr}(w), \Gamma_{sd}
2: Initialize empty list Add, define set \mathcal{I} indexing the
      lightpaths stored in stack \Gamma_{curr}(w).
3: for all entries \Gamma_{sd}(w'): 1 \leq w' \leq len(\Gamma_{sd}) such that
      \Gamma_{sd}.C_{occ}(w') = \Gamma_{curr}.C_{occ}(w) and \Gamma_{sd}.\phi_{nn'o}(w')
      +\Gamma_{curr}.\phi_{tot,nn'o}(w) \leq 1 \ \forall \ (n,n') \in \mathcal{E}, o \in \mathcal{O}  and
      \sum_{(n,n')} (\prod_i A_{nn'\Gamma_{curr}.k^i(w)}) \cdot A_{nn'\Gamma_{sd}.k(w')} \ge 1 do
           compute
          SP_{tot}^{new} = \sum_{(n,n'\in\mathcal{E})} \max(\max_i A_{nn'\Gamma_{curr}.k^i(w)})
          (\Gamma_{curr}.Tx^{i}(w)\cdot F_{\Gamma_{curr}.h^{i}(w)}+G), A_{nn'\Gamma_{sd}.k(w')}\cdot
          (\Gamma_{sd}.Tx(w')\cdot F_{\Gamma_{sd}.h(w')}+G))
          if SP_{tot}^{new} < \Gamma_{curr}.SP_{tot}(w) + \Gamma_{sd}.SP(w') then
5:
             RSP \leftarrow \frac{\Gamma_{curr}.SP_{tot}(w) + \Gamma_{sd}.SP(w') - SP_{tot}^{new}}{\Gamma_{curr}.SP_{tot}(w) + \Gamma_{sd}.SP(w')}
\Phi_{tot}^{new} \leftarrow \Gamma_{curr}.\Phi_{tot}(w) + \Gamma_{sd}.\Phi(w')
6:
7:
             CT_{tot}^{new} \leftarrow \Gamma_{curr}.CT_{tot}(w) + \Gamma_{sd}.CT(w')
8:
9:
             Append to list Add entry
            [[(s_i, d_i), \Gamma_{curr}.k^i(w), \Gamma_{curr}.m^i(w), \Gamma_{curr}.h^i(w),
           \Gamma_{curr}.C^{i}(w), \Gamma_{curr}.SP^{i}(w)): i \in \mathcal{I}, (s, d),
           \Gamma_{sd}.k(w'), \Gamma_{sd}.m(w'), \Gamma_{sd}.h(w'), \Gamma_{sd}.C(w'),
           \Gamma_{sd}.SP(w')), C_{occ}, SP_{tot}^{new}, CT_{tot}^{new}, RSP, \Phi_{tot}^{new}]
            end if
10:
11: end for
12: return Add
```

mode group is used for transmission in at most one entry on every link (i.e.,  $\sum_{i} \Gamma_{s_i d_i} . \phi_{nn'o}(w^i) \leq 1 \ \forall \ (n, n') \in \mathcal{E}, o \in \mathcal{O}$ ), then those lightpaths could share the same optical channel over their common links (Alg. 3, lines 3-11). In that case, the overall spectrum occupation  $SP_{tot}$  of the two (resp. three) considered lightpaths is recomputed, assuming that the spectrum width of the shared channel is equal to  $\max_{i \in \mathcal{I}}$  $A_{nn'\Gamma_{s_id_i}.k(w^i)} \cdot (\Gamma_{s_id_i}.Tx(w^i) \cdot F_{\Gamma_{s_id_i}.h(w^i)} + G)$  (i.e., to the maximum channel width among those stored in the two - resp. three - considered entries) for every shared link (line 4). Note that such value may differ from link to link, since not all the links are traversed by every lightpath being stacked. If  $SP_{tot}$ is smaller that the sum of the spectrum occupations of the lightpaths  $\sum_{i \in \mathcal{I}} \Gamma_{s_i d_i} . SP(w^i)$  (assuming that each of them is assigned to a different channel), it means that stacking the lightpaths over the same channel saves some spectral resources (Alg. 3, line 5). In such case, the spectrum usage relative reduction RSP, the total cost  $CT_{tot}$  of the transceiver pairs installed along each stacked lightpath and the indicator  $\Phi_{tot}$  of mode groups occupation in every link of the stack are computed (Alg. 3, lines 6-8). Finally the entry  $[(s_i, d_i), \Gamma_{s_i d_i}.k(w^i),$  $\Gamma_{s_i d_i} . m(w^i), \Gamma_{s_i d_i} . h(w^i), \Gamma_{s_i d_i} . c(w^i), \Gamma_{s_i d_i} . SP(w^i) : i \in$  $\mathcal{I}$ ],  $c_{occ}$ ,  $SP_{tot}$ ,  $CT_{tot}$ , RSP,  $\Phi_{tot}$ ] is appended to the list St, which stores the feasible lightpath stacks (Alg. 3, line 9). At the end, the routine returns the list St.

Then, the current feasible stacks are copied in the list  $\Gamma_{curr}$  and examined one by one (Alg. 1, lines 14-22): for each stack, all the lightpaths between (s,d) pairs not already included in the stack are considered and the possibility of adding one of them to the stack is evaluated by means of the routine expand\_stack. The routine checks whether the existing stack and the lightpaths between (s,d) that are

#### Algorithm 5: Order.

```
1: On input of list \Gamma_{fin} and of B_{sd}
2: for all entries \Gamma_{fin}(w): 1 \leq w \leq len(\Gamma_{fin}) do
       define set \mathcal{I} indexing the lightpaths stored in stack
       if \Gamma_{fin}(w) \geq \sum_{s_i,d_i} B_{sd}.SP then
4:
5:
         delete entry \Gamma_{fin}(w)
6:
       end if
7: end for
8: If the objective is spectrum minimization, sort entries of
   \Gamma in descending order of the values in field \Gamma_{fin}.RSP
   (resp. ascending order of values in field \Gamma_{fin}.CT_{tot}
   in case of transceiver cost minimization). If multiple
   entries have the same value in field \Gamma_{fin}.RSP, sort
   them in ascending order of values in field \Gamma_{fin}.CT_{tot}
   (resp. descending order of the values in field
   \Gamma_{fin}.RSP).
9: return sorted list \Gamma_{fin}
```

# Algorithm 6: Update.

```
1: On input of list St and of entry En

2: for all entries St(w): 1 \leq w \leq len(St) do

3: for all lightpaths i stacked in entry St(w), lightpaths i' stacked in entry En do

4: if St.(s_i,d_i)(w) = En.(s_{i'},d_{i'}) or
\sum_{(n,n')\in\mathcal{E},o\in\mathcal{O}} St(w).\Phi_{tot}\cdot En.\Phi_{tot} \geq 0 then

5: eliminate entry St(w) from list St

6: end if

7: end for

8: end for

9: return list St
```

candidate for addition to the stack share at least one link (i.e.,  $\sum_{(n,n')\in\mathcal{E}}(\prod_{i\in\mathcal{I}}A_{nn'\Gamma_{curr}.k^i(w)})\cdot A_{nn'\Gamma_{sd}.k(w')}\geq 1$ ), if the mode groups occupied over their common links do not overlap (i.e.,  $\Gamma_{sd}.\phi_{nn'o}(w') + \Gamma_{curr}.\phi_{tot,nn'o}(w) \leq 1 \ \forall \ (n,n') \in$  $\mathcal{E}, o \in \mathcal{O}$ ), and if the total occupied mode groups along the stack and along the candidate lightpath is the same (i.e.,  $\Gamma_{sd}.C_{occ}(w') = \Gamma_{curr}.C_{occ}(w)$ ). If such three conditions are met (line 3), the routine checks whether placing the candidate lightpath in the same spectrum channel of the stack leads to spectrum savings (lines 4-5) w.r.t. assigning the lightpath to a separate channel. If so, the lightpath is added to the stack, the values of  $RSP, CT_{tot}, SP_{tot}$  and  $\Phi_{tot}$  are updated and saved in the list Add (lines 6-9), which is finally returned once all the candidate lightpaths have been considered. The lists  $\Gamma_{new}$ of new stack entries generated as outputs of the routine expand\_stack are appended to a temporary list  $\Gamma_{next}$  (line 19). Once all the stacks in  $\Gamma_{curr}$  have been examined, the current list of stacks  $\Gamma_{curr}$  is copied in the final list of stacks  $\Gamma_{fin}$ , the list of new stacks is copied in  $\Gamma_{curr}$  and the procedure is repeated from the start. The loop stops either when no new stacks can be found or when the number of entries of  $\Gamma_{curr}$ exceeds a predefined threshold Th, in order to avoid excessive growth of the list  $\Gamma_{fin}$ .

# Algorithm 7: sp\_assign.

8: end for

```
    On input of list St and of set S
    for all entries St(w): 1 ≤ w ≤ len(St) do
    if no feasible assignment exists then
    algorithm halts
    else
    Assign spectrum to (stacked) lightpath(s) in entry St(w) according to a predefined assignment policy
    end if
```

Once the final list of possible stacks has been obtained, if the objective is spectrum minimization its entries are sorted in descending order of the RSP value by means of the routine order (Alg. 1, line 23). If multiple entries have the same value of  $\Gamma_{fin}.RSP$ , they are sorted in ascending order of  $\Gamma_{fin}.CT_{tot}$ . Instead, in case the objective is the minimization of the transceiver cost, the two ordering criteria are swapped (line 8). Before sorting, the routine checks whether the total spectrum occupations  $B_{sd}.SP$  calculated for each individual lightpath belonging to the stack (lines 2-7): if not, the entry is removed from the list, as assigning an individual channel to each lightpath with the most efficient combination of baud rate, modulation format and number of modes stored in  $B_{sd}$  ensures lower overall spectrum occupation.

When the order routine ends, the algorithm starts appending the first entry of the sorted list  $\Gamma_{fin}$  to the list of chosen lightpath stacks Ch (Alg. 1, line 26), the traffic requests served by the lightpaths in the stack are added to set  $\mathcal{Z}$ , which keeps track of the traffic requests served so far (Alg. 1, line 27-29), and the list of candidate stacks is updated by means of the routine update (Alg. 1, line 30). Such routine takes as input the selected lightpath stack  $\Gamma_{fin}(1)$  and the list  $\Gamma_{fin}$  and eliminates all the entries incompatible with the selected stack, i.e., the ones which contain at least one traffic request already included in the chosen lightpath stack (meaning that the condition  $St.(s_i, d_i)(w) = En.(s_{i'}, d_{i'})$  holds for at least one pair of indexes i, i') or that occupy at least one of the mode groups used by the stack on one or more of its links (i.e., if it holds that  $\sum_{(n,n')\in\mathcal{E},d\in\mathcal{O}} St(w).\Phi_{tot}\cdot En.\Phi_{tot}\geq 0$ ). The procedure is repeated until the list  $\Gamma_{fin}$  becomes empty or all the traffic requests have been served (Alg. 1, lines 25-31).

Finally, the stacks saved in the list Ch are assigned to a spectrum portion by means of the routine  $sp_assign$  (Alg. 1, line 32-34). Such routine (see Alg. 7) can implement any arbitrary spectrum assignment policy. The width of such channel on every link is determined by the number of transceiver slots required by the baud rate, modulation format, and mode group(s) combinations stored in the entries of Ch. If no commensurate spectrum portion can be assigned to the stack, the algorithm halts.

Then, using again the routine  $sp\_assign$ , a new traffic channel is allocated for each of the traffic requests  $t_{sd}$  not yet served (Alg. 1, line 35-37). The width of the spectrum channel is determined by the number of transceiver slots required by the baud rate, modulation format, and mode group(s) combina-

tion stored in  $B_{sd}$ . Again, if no feasible allocation exists, the algorithm halts.<sup>3</sup>

It is worth noting that, though the above described heuristic is designed for the fractional-joint switching scenario, it can be applied also to the full-joint switching scenario by redefining set  $\mathcal{C} = \{\alpha, \alpha \cup \beta, \alpha \cup \beta \cup \gamma\}$  or to a SMT scenario by redefining set  $\mathcal{C} = \{\alpha\}$ , and skipping lines 5-31 of Alg. 1.

#### C. Complexity Analysis

We now discuss the complexity of the solve\_RMBSA algorithm. The **for** cycle at lines 2-4 calls  $|\mathcal{T}|$  times the routine find\_c, which has complexity  $O(|\mathcal{K}_{sd}||\mathcal{M}||\mathcal{H}||\mathcal{C}|^2|\mathcal{O}||\mathcal{E}|)$ , therefore the total complexity is  $O(|\mathcal{T}||\mathcal{K}_{sd}||\mathcal{M}||\mathcal{H}||\mathcal{C}|^2|\mathcal{O}||\mathcal{E}|)$ .

The **for** cycle at lines 6-9 calls  $|\mathcal{T}|^2$  times the routine combine, which has complexity  $O((|\mathcal{K}_{sd}||\mathcal{M}||\mathcal{H}||\mathcal{C}|^2|\mathcal{O}||\mathcal{E}|)^2)$  for the case of lighpath pair stacking, therefore the total complexity is  $O((|\mathcal{T}||\mathcal{K}_{sd}||\mathcal{M}||\mathcal{H}||\mathcal{C}|^2|\mathcal{O}||\mathcal{E}|)^2)$ . Similarly, the **for** cycle at lines 10-13 has total complexity  $O((|\mathcal{T}||\mathcal{K}_{sd}||\mathcal{M}||\mathcal{H}||\mathcal{C}|^2|\mathcal{O}||\mathcal{E}|)^3)$ , since it invokes  $|\mathcal{T}|^3$  times the routine combine, which stacks lightpath triples with complexity  $O((|\mathcal{K}_{sd}||\mathcal{M}||\mathcal{H}||\mathcal{C}|^2|\mathcal{O}||\mathcal{E}|)^3)$ .

Each iteration of the **while** cycle at lines 17-22 calls  $|\mathcal{T}|$  times the routine expand\_stack for each entry of the list  $\Gamma_{curr}$ . The complexity of expand\_stack is the same of the routine find\_c, since it repeats a set of instructions for each element of the list  $\Gamma_{sd}$ , which was generated via the routine find\_c. The length of  $\Gamma_{curr}$  is  $O((|\mathcal{T}||\mathcal{K}_{sd}||\mathcal{M}||\mathcal{H}||\mathcal{C}|^2|\mathcal{O}||\mathcal{E}|)^3)$  at the first cycle iteration (as it is constructed by appending the lists  $St_2$ and  $St_3$  obtained at lines 6-13) and grows at each iteration by a multiplicative factor  $O(|\mathcal{K}_{sd}||\mathcal{M}||\mathcal{H}||\mathcal{C}|^2|\mathcal{O}||\mathcal{E}|)$ . Therefore, assuming that the number of iterations of the **while** cycle is W, the total complexity is  $O((|\mathcal{T}||\mathcal{K}_{sd}||\mathcal{M}||\mathcal{H}||\mathcal{C}|^2|\mathcal{O}||\mathcal{E}|)^{3+W})$ . The routine order invoked at line 23 first scans entry by entry the list  $\Gamma_{fin}$ , possibly deleting them, with complexity  $O((|\mathcal{T}||\mathcal{K}_{sd}||\mathcal{M}||\mathcal{H}||\mathcal{C}|^2|\mathcal{O}||\mathcal{E}|)^{3+W})$ , then sorts a subset of non deleted entries of  $\Gamma_{fin}$ . Since the amount of non-deleted entries is expected to be significantly lower than the total list size, the complexity of the sort operation can be safely assumed as lower than the complexity of the initial list scan.

The **while** cycle at lines 25-31 operates at most |T| cycles. In each cycle the list  $\Gamma_{fin}$  is scanned entry by entry, possibly deleting some of them. Therefore, the complexity of the **while** cycle can again be safely assumed as lower than the complexity of the **while** cycle at lines 15-22.

Finally, at lines 32-37 the sp\_assign is globally invoked  $|\mathcal{T}|$  times. The complexity of this phase is thus  $O(|\mathcal{T}|S_{ass})$ , where  $S_{ass}$  is the complexity of the implemented spectrum assignment policy.

In conclusion, the complexity of the whole algorithm is  $O((|T||\mathcal{K}_{sd}||\mathcal{M}||\mathcal{H}||\mathcal{C}|^2|\mathcal{O}||\mathcal{E}|)^{3+W} + |T|S_{ass})$ . Note that, to obtain a safe upper bound, the stop condition of the **while** cy-

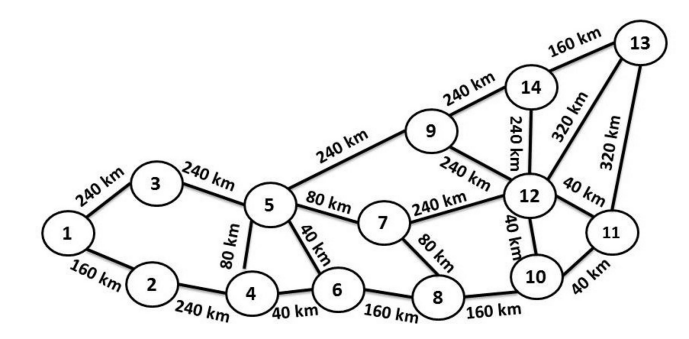


Fig. 5. Japan network topology.

cle at lines 15-22 can be replaced by a condition imposing a fixed number of iterations.<sup>4</sup> Since by definition  $|\mathcal{T}| \leq |\mathcal{N}|^2$ ,  $|\mathcal{E}| \leq |\mathcal{N}|^2$  and  $|\mathcal{C}| \leq 2^{|\mathcal{O}|}$ , whereas the cardinality of the sets of candidate lightpaths  $K_{sd}$ , modulation formats  $\mathcal{M}$  and of the baud rates  $\mathcal{H}$  are typically in the order of a few units, the complexity of the algorithm can be further approximated as  $O((|\mathcal{N}|^4|\mathcal{O}|2^{2|\mathcal{O}|})^{3+W} + |\mathcal{N}|^2 S_{ass})$ .

#### V. ILLUSTRATIVE NUMERICAL RESULTS

# A. Optimization Scenarios

The RMBSA problem is solved over two network topologies: i) a ring network with 8 nodes and radius  $R=10,\,50$  or 100 km; ii) the Japan network tepology in Fig. 5, with links scaled by a factor  $\omega=1,0.5,0.25$ . The traffic matrix (with overall traffic volume of 10, 50 or 100 Tbps) is either all-to-all (i.e. each node sends/receives traffic from every other node) or one-to-all (i.e., traffic is either originated or terminated by one node, which communicates with all the remaining ones). The available spectrum per link is S=4 THz, subdivided in 320 slices of F=12.5 GHz, with G=F. We compare five different scenarios:

- single mode transmission (SMT);
- few-mode transmission with low-complexity MIMO transceivers and full-joint switching (FMT-L-J);
- few-mode transmission with full-MIMO transceivers and full-joint switching (FMT-H-J);
- few-mode transmission with low-complexity MIMO transceiver and fractional-joint switching (FMT-L-F);
- few-mode transmission with low-complexity MIMO transceiver and fractional-joint switching without node traversal reach penalties (FMT-L-F\*).<sup>5</sup>

We set  $p_x = 3$ , Th = 10000 and implement first-fit spectrum assignment in the routine sp\_assign. The RMBSA heuristic was implemented in MATLAB and run over a machine with an Intel i7 processor. Depending on the scenario, the running times varied from a few tens of seconds (for the SMT scenario in the ring topology) to a few hours (for the FMT-L-F\* scenario in the Japan topology).

 $<sup>^3</sup>$ Note that, though our algorithm is designed for a greenfield deployment under static traffic conditions, it could also be applied for brownfield deployment, i.e. assuming the presence of some already-existing requests that cannot be re-routed nor stacked and for which transmission parameters (e.g. baud rate and modulation format) cannot be modified. In such case, set  $\mathcal T$  shall include only the batch of new requests and the routine  $sp_assign$  should avoid spectrum allocation over spectrum portions already occupied by the existing traffic connections.

<sup>&</sup>lt;sup>4</sup>Note that the  $O(|\mathcal{T}||\mathcal{E}|)^3$  factor is due to the **for all** cycle at line 3 of the combine routine to identify triplets of lightpaths sharing at least one link. The number of such triplets strongly depends on the sparsity of the network topology and is typically much lower than  $(|\mathcal{T}||\mathcal{E}|)^3$ . For a fixed network graph, these triplets can be computed offline and stored in a list, to avoid recomputation at every execution of the algorithm.

<sup>&</sup>lt;sup>5</sup>This scenario is introduced in anticipation of future technological improvements of mode combination/separation technologies with low losses.

| _      |          |                                      |         |          |            |         |         |                          |                       |         |                          |         |         |                          |         |         |                          |         |         |
|--------|----------|--------------------------------------|---------|----------|------------|---------|---------|--------------------------|-----------------------|---------|--------------------------|---------|---------|--------------------------|---------|---------|--------------------------|---------|---------|
|        |          |                                      |         | Minimiza | tion o     | $f S_o$ |         |                          | Minimization of $C_t$ |         |                          |         |         |                          |         |         |                          |         |         |
| P (lcm |          | m) one-to-all<br>SMT FMT-L-J FMT-L-F |         |          | all-to-all |         |         | one-to-all, $\delta = 1$ |                       |         | all-to-all, $\delta = 1$ |         |         | one-to-all, $\delta = 0$ |         |         | all-to-all, $\delta = 0$ |         |         |
| 1      | K (KIII) | SMT                                  | FMT-L-J | FMT-L-F  | SMT        | FMT-L-J | FMT-L-F | SMT                      | FMT-L-J               | FMT-L-F | SMT                      | FMT-L-J | FMT-L-F | SMT                      | FMT-L-J | FMT-L-F | SMT                      | FMT-L-J | FMT-L-F |
|        | 10       | 0                                    | 0       | 0        | 0          | 0       | 4.6     | 0                        | 0                     | 0       | 0                        | 0       | 0       | 0                        | 0       | 0       | 0                        | 0       | 0       |
|        | 50       | 0                                    | 0       | 0        | 0          | 0       | 3.1     | 0                        | 0                     | 0       | 0                        | 0       | 0       | 0                        | 0       | 0       | 0                        | 0       | 0       |
| - [    | 100      | 0                                    | 0       | 0        | 0          | 0       | 0       | 0                        | 0                     | 0       | 0                        | 0       | 0       | 0                        | 0       | 0       | 0                        | 0       | 0       |

TABLE III GAP (%) W.R.T. OPTIMAL  $S_o$  and  $C_t$  for the Ring Topology With 10 Tbps Traffic

# B. Comparison to Optimal Results

We start comparing the performance of the solve\_RMBSA algorithm to the optimal solution obtained by solving the ILP formulation provided in [2], in terms of spectrum occupation  $(S_o, \text{ expressed in THz})$  and overall transceiver cost  $(C_t)$ .

Due to the limited scalability of the ILP model, we focus on a ring topology with 10 Tbps total traffic and consider the SMT, FMT-L-J and FMT-L-F scenarios (i.e., the ones for which optimal results are provided in [2]). Note that, to allow for a fair comparison to the results reported in [2], in this case the cost of low-complexity MIMO transceivers was modelled as  $\Delta \left(1 + ((\sum_{o \in C} \rho_o) - 1)\delta\right)$ , as done in [2], but in the rest of the Section transceivers costs will be modelled as discussed in Section III.

Percentual gaps w.r.t. optimal solutions are reported in Table III. In the SMT and FMT-L-J scenarios, when minimizing  $S_o$ , the solve\_RMBSA heuristic always finds optimal solutions. Differently, In the FMT-L-F scenario, the effect of stacking lightpaths due to channel sharing emerges. However, gaps w.r.t. the optimal spectrum occupation are always below 6%. Conversely, when minimizing  $C_t$ , results obtained with the solve RMBSA algorithm are always optimal. Note also that, when  $\delta = 1$  (i.e., when the transceiver cost grows linearly with the number of used modes) it is preferable to use only group  $\alpha$ , as it enables the usage of more spectrally efficient modulation formats w.r.t. groups  $\beta$  and  $\gamma$  and consequently it reduces the number of transceivers required to serve a given traffic amount. Differently, when  $\delta = 0$  (i.e., when the cost of a FMT transceiver is assumed to be equal to that of a SMT transceiver, regardless to the number of occupied modes), traffic requests may be served using multiple mode groups, possibly reducing the required optical channel bandwidth w.r.t. SMT, without increasing the overall transceiver costs.

# C. Evaluating the Benefits of FMT

To quantify the savings achieved by different FMT scenarios with respect to SMT, we run experiments minimizing either  $S_o$  or  $C_t$  using our heuristic algorithm for SMT, FMT-L-J, FMT-H-J, FMT-L-F and FMT-L-F\* and we report in Tables IV and V the overall spectrum occupation (i.e., the sum of the spectrum slots occupied over every link, in THz) and the total transceiver costs (assuming the cost  $\Delta$  of a SMT transceiver as unit). We start commenting on results with full-joint switching (-J). Results show that, when minimizing  $S_o$ , in FMT-H-J, full-MIMO trasceivers enable very high spectrum savings (up to 72% less spectrum than in SMT in the ring topology, and up to 68% in the Japan network, especially for high traffic), at the price of a sharp increase in  $C_t$  (up to more than 8 times higher than SMT in the ring topology and 20 times higher in the Japan network, for low traffic). Spectrum savings achievable with low-complexity

TABLE IV

COMPARISON OF SPECTRUM OCCUPATION AND TRANSCEIVER COSTS USING SMT AND FMT TECHNOLOGIES IN THE RING NETWORK, WHEN MINIMIZING  $S_{\alpha}$ 

|         |       |     |      | 5    | 0 Tbp | S    |      |      | 10   | 00 Tb <sub>1</sub> | ps   |      |
|---------|-------|-----|------|------|-------|------|------|------|------|--------------------|------|------|
|         |       | ω   | SMT  | FMT- | FMT-  | FMT- | FMT- | SMT  | FMT- | FMT-               | FMT- | FMT- |
|         |       |     |      | L-J  | H-J   | L-F  | L-F* |      | L-J  | H-J                | L-F  | L-F* |
|         |       | 10  | 16.0 | 11.2 | 6.4   | 14.0 | 10.5 | 30.4 | 16.0 | 11.2               | 26.6 | 16.0 |
| $ S_o $ | (THz) | 50  | 17.2 | 11.2 | 6.4   | 16.4 | 10.4 | 32.0 | 19.4 | 11.2               | 31.4 | 18.7 |
|         |       | 100 | 21.4 | 13.6 | 6.4   | 19.8 | 13.1 | 40.0 | 25.2 | 11.2               | 38.2 | 24.7 |
|         |       | 10  | 336  | 1120 | 2800  | 2256 | 1024 | 672  | 1680 | 5600               | 4512 | 1590 |
|         | $C_t$ | 50  | 352  | 1504 | 2800  | 2064 | 1408 | 704  | 3648 | 5600               | 4128 | 3324 |
|         |       | 100 | 496  | 2288 | 2800  | 2304 | 2172 | 976  | 5376 | 5600               | 4608 | 4584 |

TABLE V Comparison of Spectrum Occupation and Transceiver Costs Using SMT and FMT Technologies in the Japan Network, When Minimizing  $S_{\alpha}$ 

|             |      |      |      | 0 Tbp |      |      |      |      | 00 Tb <sub>1</sub> | F    |      |
|-------------|------|------|------|-------|------|------|------|------|--------------------|------|------|
|             | ω    | SMT  | FMT- | FMT-  | FMT- | FMT- | SMT  | FMT- | FMT-               | FMT- | FMT- |
|             |      |      |      |       |      | L-F* | l .  |      |                    | L-F  |      |
|             | 0.25 | 24.0 | 20.4 | 16.5  | 24.3 | 20.3 | 42.5 | 34.4 | 16.5               | 43.0 | 33.5 |
| $S_o$ (THz) | 0.5  | 29.5 | 23.4 | 16.5  | 28.8 | 23.1 | 49.1 | 41.1 | 16.9               | 52.3 | 40.1 |
|             | 1    | 35.8 | 31.2 | 16.5  | 34.7 | 30.8 | 60.7 | 56.5 | 19.4               | 64.0 | 55.7 |
|             | 0.25 | 442  | 1668 | 9100  | 1852 | 1560 | 884  | 2960 | 9100               | 3678 | 2892 |
| $C_t$       | 0.5  | 592  | 1858 | 9100  | 1884 | 1754 | 1126 | 3552 | 9100               | 3616 | 3496 |
|             | 1    | 696  | 2100 | 9100  | 1720 | 1960 | 1270 | 4094 | 9200               | 3488 | 3954 |

MIMO transceivers (FMT-L-J) are lower, yet still significant (up to 37% in the ring topology and up to 20% in the Japan network), with  $C_t$  3 to 4 times higher than in SMT. In the fractional-joint switching scenario (-F), FMT-L-F ensures  $S_o$  reductions up to 13% w.r.t. SMT in small topologies, whereas  $S_o$  can even become slightly higher than in SMT for high traffic and large topologies, mainly due to node-traversal impairments, which prevent the adoption of highly efficient modulation formats.  $C_t$  is also 4 to 8 times higher than in SMT. Conversely, FMT-L-F\* obtains remarkable savings (up to 47%) in all traffic and network settings, with transceiver cost slightly lower than in the FMT-L-J scenario. Note that transmission reaches in the FMT-L-J and FMT-L-F\* scenarios are identical, therefore the additional savings in  $S_o$  achieved with FMT-L-F\* w.r.t. FMT-L-J are due to the benefits of channel sharing.

Finally, Tables VI and VII report the comparison of  $S_o$  and  $C_t$  obtained when minimizing  $C_t$ , for either  $\delta=1$  or 0. Results show that, when minimizing transceiver costs, FMT is never advantageous, as it leads to the same values of both  $C_t$  and  $S_o$  w.r.t. SMT (or even higher in the case of FMT-L-F). However, FMT-L-J and FMT-L-F\* with  $\delta=0$  ensure the same performance of SMT in terms of  $C_t$  and lead to some reductions (up to 20% in small topologies) in  $S_o$  without increasing  $C_t$ , thus showing the advantage of the adoption of low-complexity MIMO transceivers. Finally, FMT-H-J with  $\delta=0$  obtains significant reductions in both spectrum occupation and transceiver cost w.r.t. SMT. This is due to the fact that, under such assump-

TABLE VI COMPARISON OF SPECTRUM OCCUPATION AND TRANSCEIVER COSTS USING SMT AND FMT TECHNOLOGIES IN THE RING NETWORK, WHEN MINIMIZING  $C_t$ , FOR TWO DIFFERENT VALUES OF THE COST PARAMETER  $\delta$ 

|             |   |      |      | 5    | 0 Tbp | os   |      |      | 1    | 00 Tb | ps   |      |
|-------------|---|------|------|------|-------|------|------|------|------|-------|------|------|
|             | δ | ω    | SMT  | FMT- | FMT-  | FMT- | FMT- | SMT  | FMT- | FMT-  | FMT- | FMT- |
|             |   |      |      | L-J  | H-J   | L-F  | L-F* |      | L-J  | H-J   | L-F  | L-F* |
|             | 1 | 10   | 16.0 | 16.0 | 16.0  | 22.0 | 16.0 | 30.4 | 30.4 | 30.4  | 37.6 | 30.4 |
|             | 0 | 10   | 10.0 | 10.0 | 6.4   | 22.0 | 14.4 | 30.4 | 16.0 | 11.2  | 37.0 | 16.0 |
| $S_o$ (THz) | 1 | 50   | 17.2 | 17.2 | 17.2  | 23.2 | 17.2 | 32.8 | 32.8 | 32.8  | 40.0 | 32.8 |
| 00 (1112)   | 0 | 30   | 17.2 | 17.2 | 6.4   | 23.2 | 17.2 | 32.0 | 31.0 | 11.2  | 70.0 | 31.0 |
|             | 1 | 100  | 23.2 | 23.2 | 23.2  | 25.6 | 23.2 | 41.8 | 41.8 | 41.8  | 46.6 | 41.8 |
|             | 0 | 100  | 20.2 |      | 6.4   | 20.0 |      |      |      | 11.2  |      | 1110 |
|             | 1 | 10   | 336  | 336  | 336   | 432  | 336  | 672  | 672  | 672   | 816  | 672  |
|             | 0 | - "  |      |      | 112   |      |      |      |      | 224   |      |      |
| $C_t$       | 1 | 50   | 352  | 352  | 352   | 464  | 352  | 704  | 704  | 704   | 880  | 704  |
| - 0         | 0 |      |      |      | 112   |      |      |      |      | 224   |      |      |
|             | 1 | 100  | 464  | 464  | 464   | 512  | 464  | 880  | 880  | 880   | 960  | 880  |
|             | 0 | _ 50 |      |      | 112   |      |      | - 30 |      | 224   |      |      |

TABLE VII

Comparison of Spectrum Occupation and Transceiver Costs Using SMT and FMT Technologies in the Japan Network, When Minimizing  $C_t$ , for Two Different Values of the Cost Parameter  $\delta$ 

|      |        |        |      |      | 5    | 0 Tbp      | S    |      |      | 10   | 00 Tb       | ps   |      |
|------|--------|--------|------|------|------|------------|------|------|------|------|-------------|------|------|
|      |        | δ      | ω    | SMT  | FMT- | FMT-       | FMT- | FMT- | SMT  | FMT- | FMT-        | FMT- | FMT- |
|      |        |        |      |      | L-J  | H-J        | L-F  | L-F* |      | L-J  | H-J         | L-F  | L-F* |
|      |        | 1      | 0.25 | 24.0 | 24.0 | 24.0       | 32.0 | 24.0 | 44.5 | 44.5 | 44.5        | 54.9 | 44.5 |
|      |        | 0      | 0.23 | 24.0 | 22.0 | 16.5       | 27.9 | 21.0 | 44.3 | 42.8 | 16.5        | 50.4 | 40.4 |
| G .  | (THz)  | 1      | 0.5  | 29.5 | 29.5 | 29.5       | 34.4 | 29.5 | 51.8 | 51.8 | 51.8        | 59.1 | 51.8 |
| 00 ' | (1112) | 0      | 0.5  | 29.3 | 26.8 | 16.5       | 32.7 | 26.3 | 51.0 | 51.2 | 16.9        | 57.1 | 49.9 |
|      |        | 1      | 1    | 35.8 | 35.8 | 35.8       | 38.2 | 35.8 | 61.6 | 61.6 | 61.6        | 68.3 | 61.6 |
|      |        | 0      | 1    | 33.0 | 34.9 | 16.5       | 37.7 | 34.6 | 01.0 | 61.3 | 19.4        | 68.0 | 60.6 |
|      |        | 1      | 0.25 | 442  | 442  | 442<br>364 | 632  | 442  | 806  | 806  | 806<br>364  | 1016 | 806  |
|      | $C_t$  | 1      | 0.5  | 592  | 592  | 592<br>364 | 648  | 592  | 960  | 960  | 960<br>364  | 1084 | 960  |
|      |        | 1<br>0 | 1    | 696  | 696  | 696<br>364 | 736  | 696  | 1170 | 1170 | 1170<br>368 | 1316 | 1170 |

tions, the cost of a full MIMO transceiver results to be the same as that of a SMT transceiver.

# D. Cost Assessment of FMT Deployments

Based on results in Tables IV–VII, we now evaluate the network deployment costs in terms of transceivers and dark fiber leasing expenditures (i.e., costs due to spectrum occupation), depending on the transmission (full-MIMO vs. low-complexity MIMO) and switching (full-joint vs fractional-joint) technologies in use. According to a recent report [32], dark fiber leasing expenditures in metro areas vary in the range between 15 USD and 6000 USD per fiber per month per mile (depending on whether construction costs are included), plus a yearly maintenance fee. Let us indicate the leasing cost per fiber per month per mile as  $\eta$  and the yearly maintenance fee as  $\mu$ . We introduce a parameter  $\nu$  indicating the ratio of the cost of 1 THz bandwidth per km per 10 years leasing time to the cost of one SMT transceiver, which can be computed as:

$$\nu = \frac{\left(\frac{\eta}{4 \cdot 1.61} \cdot 12 + \mu\right) \cdot 10}{\Delta}$$

assuming that the total bandwidth of a fiber is 4 THz and considering a factor 1.61 for conversion between miles and kms. Under assumption that one SMT transceiver costs 10000 USD, realistic

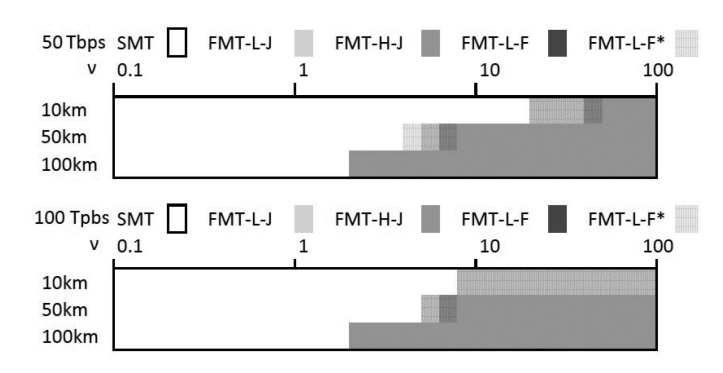


Fig. 6. Deployment cost assessment in the ring network topology.

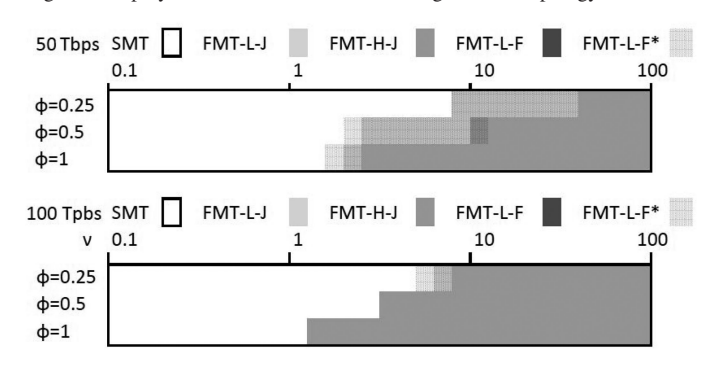


Fig. 7. Deployment cost assessment in the Japan network topology.

values of  $\nu$  are expected to vary in the range between 0.1 and 100 (e.g.,  $\nu = 1$  indicates that leasing 1 THz bandwidth over 1 km for 10 years yields a 10000 USD expenditure). We then evaluate the deployment costs of the five considered settings (i.e., SMT, FMT-L-J, FMT-H-J, FMT-L-F and FMT-L-F\*) and report the least expensive one in Figs. 6–7, depending on the value of  $\nu$ , on the overall traffic load and on the network topology and size. Results show that, when  $\nu < 1$  (i.e., when transceiver costs are predominant), SMT is always the most convenient transmission technology, as it ensures significantly lower transceiver usage w.r.t. FMT. Transition from SMT to FMT occurs, in most of the cases, for values of  $\nu$  between 1 and 10 (with  $\nu$  closer to 1 for bigger topologies). For  $\nu > 10$  (i.e., when fiber leasing expenditures dominate transceiver costs) FMT-H-J achieves the lowest deployment costs, as it ensures the lowest overall spectrum occupation due to the long reaches and high spectral efficiency of full-MIMO transmission. Conversely, for values of  $\nu$  close to the transition point between SMT and FMT, the advantage of low-complexity MIMO transceivers emerges (especially for low traffic loads), when a full-joint switching mechanism is adopted: in such setting, less spectrum is occupied w.r.t. SMT and the transceiver cost is lower than in FMT-H-J, thus achieving the best cost trade-off. Note that, if the FMT-L-F\* setting were enabled by future advancements in the switching technologies, such setting (identified in Figs. 6–7 by a shaded pattern) would outperform FMT-L-J, since it would benefit of the additional spectrum flexibility of the fractional-joint switching scenario (which allows for channel stacking) while achieving the same

<sup>&</sup>lt;sup>6</sup>Note that, when  $\nu < 1$  transceiver minimization criteria are applied by the heuristic algorithm, whereas when  $\nu \geq 1$ , spectrum minimization criteria are adopted. In all settings,  $\delta = 1$  is assumed for the computation of FMT transceiver costs.

transmission reaches of FMT-L-J. Conversely, FMT-L-F is never advantageous, as node traversal penalties introduced by the fractional-joint switching scenario cause consistent penalization of transmission reaches, leading to consistently higher spectrum utilization and higher transceiver costs than in FMT-L-J.

#### VI. CONCLUSIONS

This paper presents a scalable heuristic for routing, baud rate, modulation format, mode and spectrum assignment in flexible optical networks with few-mode transmission. The heuristic can be flexibly adapted to minimize spectrum usage or the transceivers cost, and can solve the problem under five different switching and transmission scenarios. We demonstrate that solutions obtained with our heuristic closely approach optimal results computed with an integer linear programming formulation. Then, using the proposed heuristic and an elementary cost model based on realistic cost figures, we provide a cost comparison of the five technological scenarios, showing under which circumstances (in terms of network size and spectrum/transceiver cost ratio) each scenario lead to minimum cost.

#### REFERENCES

- G. M. Saridis, D. Alexandropoulos, G. Zervas, and D. Simeonidou, "Survey and evaluation of space division multiplexing: From technologies to optical networks," *IEEE Commun. Surv. Tuts.*, vol. 17, no. 4, pp. 2136–2156, Oct.–Dec. 2015.
- [2] C. Rottondi, P. Boffi, P. Martelli, and M. Tornatore, "Routing, modulation format, baud rate and spectrum allocation in optical metro rings with flexible grid and few-mode transmission," *J. Lightw. Technol.*, vol. 35, no. 1, pp. 61–70, Jan. 2017.
- [3] M. Klinkowski, P. Lechowicz, and K. Walkowiak, "Survey of resource allocation schemes and algorithms in spectrally-spatially flexible optical networking," Opt. Switch. Netw., vol. 27, pp. 58–78, 2018.
- [4] C. Rottondi and M. Tornatore, "An inter-modal-coupling-aware heuristic algorithm for routing, spectrum and mode assignment in few-mode optical networks," in *Proc. Adv. Photon. (BGPP, IPR, NP, NOMA, Sensors, Netw., SPPCom, SOF)*, 2018, Paper NeTh1F.2. [Online]. Available: http://www. osapublishing.org/abstract.cfm?URI=Networks-2018-NeTh1F.2
- [5] D. Siracusa, F. Pederzolli, D. Klonidis, V. Lopez, and E. Salvadori, "Resource allocation policies in SDM optical networks," in *Proc. Int. Conf. Opt. Netw. Des. Model.*, 2015, pp. 168–173.
- [6] D. Klonidis et al., "Spectrally and spatially flexible optical network planning and operations," *IEEE Commun. Mag.*, vol. 53, no. 2, pp. 69–78, Feb. 2015.
- [7] D. M. Marom and M. Blau, "Switching solutions for WDM-SDM optical networks," *IEEE Commun. Mag.*, vol. 53, no. 2, pp. 60–68, Feb. 2015.
- [8] F. Pederzolli, D. Siracusa, J. M. Rivas-Moscosoy, B. Shariati, E. Salvadori, and T. Ioannis, "Spatial group sharing for SDM optical networks with joint switching," in *Proc. Int. Conf. Opt. Netw. Des. Model.*, Cartagena, 2016, pp. 1–6.
- [9] B. Shariati et al., "Impact of spatial and spectral granularity on the performance of SDM networks based on spatial superchannel switching," J. Lightw. Technol., vol. 35, no. 13, pp. 2559–2568, Jul. 2017.
- [10] P. S. Khodashenas et al., "Comparison of spectral and spatial superchannel allocation schemes for SDM networks," J. Lightw. Technol., vol. 34, no. 11, pp. 2710–2716, Jun. 2016.
- [11] B. Shariati et al., "Evaluation of the impact of different SDM switching strategies in a network planning scenario," in Proc. Opt. Fiber Commun. Conf., 2016, Paper Tu2H.4.

- [12] D. Siracusa et al., "Spectral vs. spatial super-channel allocation in SDM networks under independent and joint switching paradigms," in Proc. 41st Eur. Conf. Exhib. Opt. Commun., Valencia, Spain, 2015, pp. 1–3.
- [13] Y. Li, N. Hua, and X. Zheng, "Routing, wavelength and core allocation planning for multi-core fiber networks with MIMO-based crosstalk suppression," in *Proc. Opto-Electron. Commun. Conf.*, 2015, pp. 1–3.
- [14] Y. Li, N. Hua, and X. Zheng, "CapEx advantages of multi-core fiber networks," *Photon. Netw. Commun.*, vol. 31, pp. 228–238, 2016.
- [15] A. Muhammad, G. Zervas, D. Simeonidou, and R. Forchheimer, "Routing, spectrum and core allocation in flexgrid SDM networks with multi-core fibers," in *Proc. Int. Conf. Opt. Netw. Des. Model.*, 2014, pp. 192–197.
- [16] A. Muhammad, G. Zervas, G. Saridis, E. Salas, D. Simeonidou, and R. Forchheimer, "Flexible and synthetic SDM networks with multi-core-fibers implemented by programmable ROADMs," in *Proc. Eur. Conf. Opt. Commun.*, Sep. 2014, pp. 1–3.
- [17] S. Yin, S. Huang, B. Guo, X. Li, C. Wang, and H. Huang, "Inter-core crosstalk aware routing, spectrum and core allocation in multi-dimensional optical networks," in *Proc. Opto-Electron. Commun. Conf. Photon. Global Conf.*, Jul. 2017, pp. 1–4.
- [18] Y. Li, N. Hua, X. Zheng, and G. Li, "CapEx advantages of few-mode fiber networks," in *Proc. Opt. Fiber Commun. Conf.*, 2015, Paper Th2A 43
- [19] S. Fujii, Y. Hirota, H. Tode, and K. Murakami, "On-demand spectrum and core allocation for reducing crosstalk in multicore fibers in elastic optical networks," *J. Opt. Commun. Netw.*, vol. 6, no. 12, pp. 1059–1071, 2014.
- [20] H. Tode and Y. Hirota, "Routing, spectrum and core assignment for space division multiplexing elastic optical networks," in *Proc. 16th Int. Telecommun. Netw. Strategy Planning Symp.*, Sep. 2014, pp. 1–7.
- [21] A. Muhammad, G. Zervas, and R. Forchheimer, "Resource allocation for space-division multiplexing: Optical white box versus optical black box networking," *J. Lightw. Technol.*, vol. 33, no. 23, pp. 4928–4941, Dec. 2015.
- [22] H. Huang, S. Huang, S. Yin, M. Zhang, J. Zhang, and W. Gu, "Virtual network provisioning over space division multiplexed optical networks using few-mode fibers," *IEEE/OSA J. Opt. Commun. Netw.*, vol. 8, no. 10, pp. 726–733, Oct. 2016.
- [23] R. Proietti et al., "3D elastic optical networking in the temporal, spectral, and spatial domains," *IEEE Commun. Mag.*, vol. 53, no. 2, pp. 79–87, Feb. 2015.
- [24] L. Liu, Z. Zhu, and S. Yoo, "3D elastic optical networks in temporal, spectral, and spatial domains with fragmentation-aware RSSMA algorithms," in *Proc. Eur. Conf. Opt. Commun.*, Sep. 2014, pp. 1–3.
- [25] E. Hopper and B. C. Turton, "A review of the application of meta-heuristic algorithms to 2D strip packing problems," *Artif. Intell. Rev.*, vol. 16, no. 4, pp. 257–300, 2001.
- [26] S. Randel et al., "6 × 56-Gb/s mode-division multiplexed transmission over 33-km few-mode fiber enabled by 6 × 6 MIMO equalization," Opt. Express, vol. 19, no. 17, pp. 16697–16707, 2011.
- [27] P. J. Winzer, "Making spatial multiplexing a reality," *Nature Photon.*, vol. 8, no. 5, pp. 345–348, 2014.
- [28] P. Genevaux, M. Salsi, A. Boutin, F. Verluise, P. Sillard, and G. Charlet, "Comparison of QPSK and 8-QAM in a three spatial modes transmission," *IEEE Photon. Technol. Lett.*, vol. 26, no. 4, pp. 414–417, Feb. 2014.
- [29] C. Koebele et al., "40 km transmission of five mode division multiplexed data streams at 100 Gb/s with low MIMO-DSP complexity," in Proc. Eur. Conf. Expo. Opt. Commun., 2011, Paper Th.13.C.3.
- [30] Telecommunications Standardization Sector—International Telecommunication Union, "Spectral grids for WDM applications: DWDM frequency grid," ITU-T Rec. G.694.1, Feb. 2012. [Online]. Available: http://www.itu.int
- [31] S. Ö. Arık, K.-P. Ho, and J. M. Kahn, "Optical network scaling: Roles of spectral and spatial aggregation," *Opt. Express*, vol. 22, no. 24, pp. 29868–29887, 2014.
- [32] "Dark fiber leasing considerations." 2012. [Online]. Available: http://www.ctcnet.us/DarkFiberLease.pdf. Accessed on: Dec. 1, 2018.